

Effect of optical tissue clearing on spatial resolution and sensitivity of bioluminescence imaging

E. Duco Jansen
Patrick M. Pickett
Mark A. Mackanos
John Virostko

Vanderbilt University
Department of Biomedical Engineering
VU Station B #351631
Nashville, Tennessee 37235
E-mail: duco.jansen@vanderbilt.edu

Abstract. *In vivo* bioluminescence imaging (BLI) is a powerful method of *in vivo* molecular imaging based on the use of optically active luciferase reporter genes. Although this method provides superior sensitivity relative to other *in vivo* imaging methods, spatial resolution is poor due to light scattering. The objective of this study was to use hyperosmotic agents to reduce the scattering coefficient and hence improve spatial resolution of the BLI method. A diffusing fiber tip was used to simulate an isotropic point source of bioluminescence emission (550 to 650 nm). Mouse skin was treated *in vitro* and *in vivo* with glycerol (50%, 30 min) and measurements of optical properties, and imaging photon counts were made before, during, and after application of glycerol to the skin sample. Glycerol application to mouse skin had little effect on the absorption coefficient but reduced the reduced scattering coefficient by more than one order of magnitude. This effect was reversible. Consequently, the spot size (i.e., spatial resolution) of the bioluminescence point source imaged through the skin decreased by a factor of 2 (550-nm light) to 3 (650-nm light) after 30 min. Simultaneously, an almost twofold decrease in the amount of light detected by the BLI system was observed, despite the fact that total transmission increased 1.7 times. We have shown here that multiply scattered light is responsible for both observations. We have shown that applying a hyperosmotic clearing agent to the skin of small rodents has the potential to improve spatial resolution of BLI owing to a reduction in the reduced scattering coefficient in the skin by one order of magnitude. However, reducing the scattering coefficient reduces the amount of light reaching the camera due to a reduction in the amount of multiply scattered light that reaches the camera aperture and thus reducing the sensitivity of the method. © 2006 Society of Photo-Optical Instrumentation Engineers. [DOI: 10.1117/1.2337651]

Keywords: bioluminescence; optical properties; clearing; glycerol; imaging; luciferase.

Paper 05300SSR received Oct. 6, 2005; revised manuscript received Feb. 7, 2006; accepted for publication Feb. 13, 2006; published online Aug. 25, 2006.

1 Introduction

Photoactive reporter genes allow optical imaging of *in vivo* biological activity, such as the spatial and temporal distribution of gene expression,^{1–7} host-pathogen interactions,^{8–13} tumor growth and metastasis,^{14–19} and transplant studies.^{20,21} While over 30 bioluminescence systems exist in nature, all have in common a luciferase-catalyzed oxidation of a luciferin substrate to produce light.²² Unlike fluorescence systems [i.e., green fluorescence protein (GFP)], bioluminescence imaging (BLI) requires no excitation source, which simplifies the optics involved in the imaging process, allows for detection of light emission from deeper tissues, and facilitates quantitative analysis. In addition, light emission from the chemiluminescent oxidation of the luciferin substrate emits broadband light that peaks at 563 nm (590 nm at body tem-

perature of 37°C) but spans wavelengths from 500 to 700 nm, thus allowing deep tissue penetration (on the order of several centimeters), in particular of the red parts of the emission spectrum.^{23,24} The main drawbacks to using bioluminescence for *in vivo* imaging are the extremely low intensity of light produced and the poor resolution due to tissue scattering.

Hyperosmotic agents such as glycerol, dimethyl sulfoxide (DMSO), Trazograph, polyethylene glycol, polypropylene glycol- (PPG) and polyethylene glycol- (PEG) based prepolymer mixture, and glucose have been shown to transiently clear tissue within 30 min of application in hamsters and rats^{25–27} and even in humans^{28–31} both *in vitro* and *in vivo*. Increases in transmission of up to 200% and decreases of the reduced scattering coefficient of a full order of magnitude were reported. Clearing is believed to be due to index matching of the extracellular fluid with the tissue solid components (mainly col-

Address all correspondence to E. Duco Jansen, Biomedical Engineering, Vanderbilt University, VU Station B # 351631, Nashville, TN 37235-1631; Tel: 615-343-1911; Fax: 615-343-7919; E-mail: duco.jansen@vanderbilt.edu

lagen) and dehydration due to osmotic pressure.

The objective of this study is to investigate if treating skin with a hyperosmotic agent (glycerol) in order to reduce scattering will improve the sensitivity and spatial resolution of bioluminescence imaging. This study consisted of four parts: *in vitro* measurement of tissue (i.e., mouse skin) optical properties, *in vitro* simulated BLI, *in vivo* macroscopic imaging, and *in vivo* simulated BLI.

2 Materials and Methods

2.1 *In Vitro* Optical Properties Measurement

A Perkin-Elmer Lambda-900 spectrophotometer with an integrating sphere setup was used to measure tissue optical properties. Transmission (%*T*), diffuse reflectance (%*R*), and thickness (*d*) for *in vitro* studies were measured for samples of excised albino friend virus B-type (FVB) mouse skin (2 cm × 2 cm), within 12 h of sacrifice. Prior to the optical measurements, the samples were sandwiched between two microscope slides. Care was taken that no air bubbles remained between the tissue and the slides. Thickness of skin samples was determined by measuring the thickness of the sandwich and subtracting the thickness of the microscope slides. All thickness measurements were made using a digital caliper and the average of five independent thickness measurements was used for each sample. Skin samples were then treated by soaking in glycerol baths with concentrations of 25%, 50%, and 100% for 30 min. After measuring transmission values, reflectance values and thickness, the skin samples were rehydrated by soaking in saline for 30 min. Samples were measured for transmission and reflectance again after rehydration. Values for absorption coefficient (μ_a) and reduced scattering coefficient (μ'_s) were calculated from the spectrophotometer data using an inverse adding doubling program.³² All optical property measurements were performed in triplicate (*n*=3) using samples from different mice.

2.2 *In Vitro* Simulated Bioluminescence Imaging

After determining the tissue optical properties, an *in vitro* simulated bioluminescence study was performed. The goal was to match the conditions encountered in BLI, specifically, intensity and wavelength. A tungsten white light source was bandpass filtered at 550, 600, and 650 nm [full width at half maximum (FWHM)=10 nm], then coupled into a 200- μ m diameter optical fiber with a 500- μ m diameter spherical diffusing fiber tip at the distal end, which provided an isotropic light source. The three wavelengths were chosen because luciferase-catalyzed bioluminescence has its highest intensities in the wavelength range of 500 to 700 nm.²³ The shorter wavelength components of this spectrum are attenuated by hemoglobin absorption, so the chosen wavelengths of light provided a realistic simulation of actual luciferase bioluminescence. The diffusing fiber was taped to the bottom of a petri dish (100 mm diameter). A piece (2 cm × 2 cm) of excised mouse skin was placed over the fiber tip on the bottom of the petri dish with the epidermal side facing the fiber and the subdermal side facing up. The sample was held in place by a metal retaining ring with an aperture large enough (1.5 cm diameter) such that it did not block any light. For all experiments, a constant volume of 25 ml of glycerol solution

of 25%, 50%, or 100% concentration (v/v) was added to the petri dish such that a layer of glycerol, roughly 3-mm high was overlying the skin sample. The entire assembly of petri dish, fiber, skin sample, and glycerol was placed in the light-tight imaging chamber. The fiber was guided into the chamber via a double baffled black rubber seal to avoid stray light from entering the imaging chamber. Images were then taken with a liquid nitrogen-cooled, back-thinned, back-illuminated, deep depletion charge-coupled device (CCD) camera (Roper EEV 1300 × 1340). Background subtraction was performed on all images as a means of noise reduction. Image integration times of 5 s were used and no on-chip binning was used. The setup is summarized in Fig. 1. Intensity is reported as the integrated pixel intensity for a defined area of a CCD image at a specific time point relative to the first time point for each wavelength. Spot size is defined as the width of the section of the cross-sectional intensity profile where values are greater than a pre-defined threshold (100 photon counts).

Images were taken of the fiber alone, the fiber with overlying skin, and the fiber with overlying skin submerged in glycerol (time sequence). To minimize the effect of biological variation among skin samples, the experiment was designed to perform all three wavelengths in a single skin sample. This was accomplished by letting the camera controller take an image every 40 s for a duration of 5 s while rotating the three bandpass filters in front of the white light source every 40 s to provide time points for each wavelength in 2-min intervals.

2.3 *In Vivo* Macroscopic Imaging

Live mice were treated with transdermal glycerol injections and imaged over time. Eight-week old, female albino FVB mice were anesthetized with 0.015 ml/g body weight of a mixture of ketamine (6 mg/ml) and xylazine (0.6 mg/ml) given intraperitoneally. Administration of glycerol was accomplished by inserting a 21-gauge needle subdermally in the animal's dorsal side, then lifting up and entering the dermis from the subcutaneous side. Approximately 0.2 ml of either 50% or 100% glycerol were injected in 0.05- or 0.1-ml increments. Images of the skin in the live mouse were taken with a digital camera coupled to a 10× operating microscope before, immediately after, 30 min, 60 min and 24 h post-glycerol application.

2.4 *In Vivo* Simulated Bioluminescence Imaging

The *in vivo* simulated bioluminescence experiment used a similar setup to the *in vitro* simulated bioluminescence experiment (Fig. 1). The diffusing fiber was placed subdermally in the mouse after glycerol was injected transdermally. The injection procedure described for the *in vivo* macroscopic imaging study was used. Based on the findings of the *in vitro* study, the 600-nm wavelength light and 50% glycerol concentration were used. Photon counting images were taken at *t*=0 (pretreatment), 15, and 30 min.

3 Results

Figures 2 show the increase in transmission [Fig. 2(a)] and decrease in diffuse reflectance [Fig. 2(b)], respectively, after treating native skin with 50% glycerol for 30 min (each line represents the average of three independent measurements). These figures also show that transmission and reflectance re-

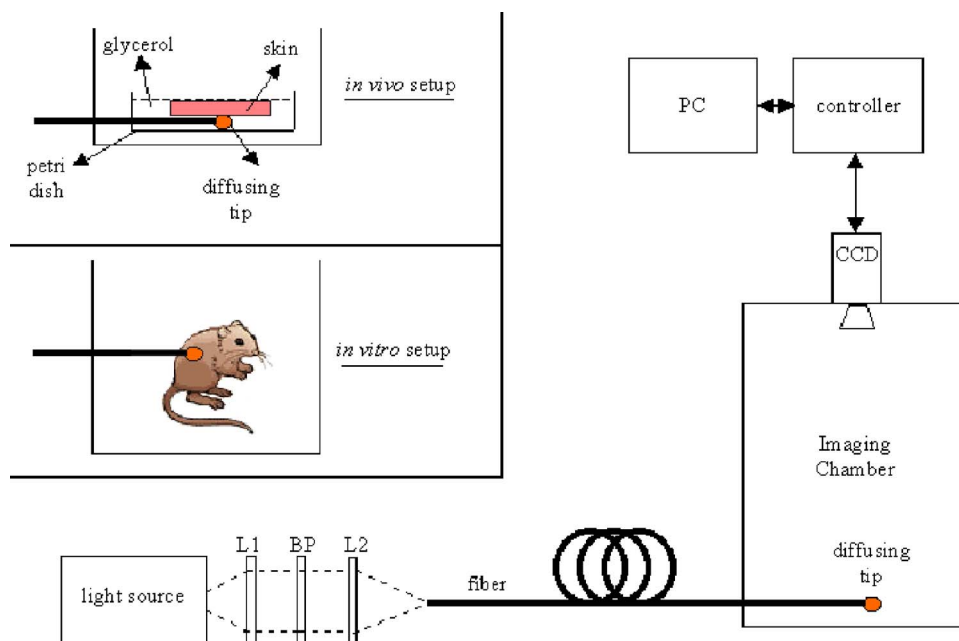
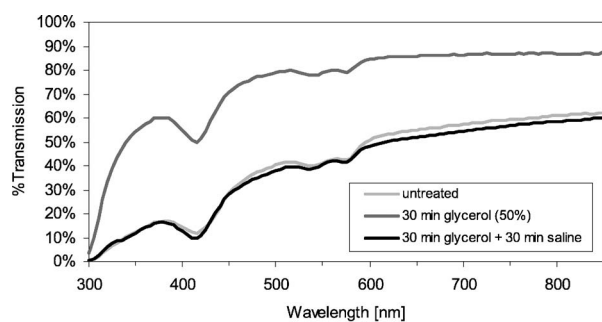
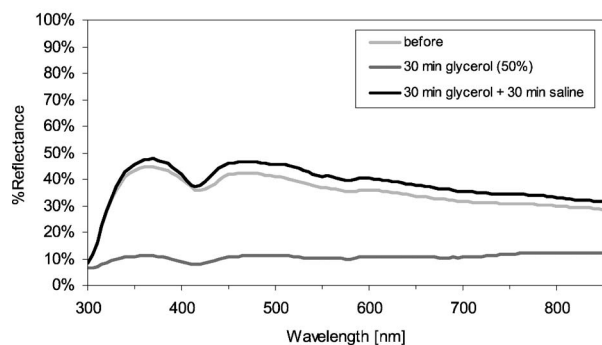


Fig. 1 Schematic of the experimental setup. A bioluminescence point source was simulated by using bandpass filtered light (550 nm, 600 nm, or 650 nm) delivered via a 200- μm fiber to an isotropic diffuser tip. The same setup was used for *in vitro* (top left inset) and *in vivo* (bottom left inset) experiments.



(a)



(b)

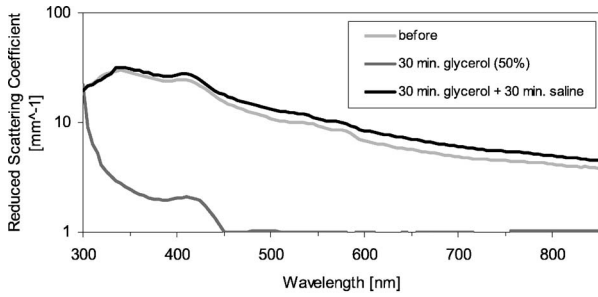
Fig. 2 Total transmission (a) and reflectance (b) measurements of *in vitro* normal skin, glycerol treated skin (50%, 30 min), and skin treated with glycerol for 30 min then placed in saline for 30 min. In the spectral range of interest (550 to 650 nm), the total transmission increases (nearly two-fold) and the diffuse reflectance decreases (threefold to fourfold) due to glycerol application. Each line represents the average of three independent measurements ($n=3$).

turn to approximately their pretreatment values after rehydration with saline for 30 min. The reduced scattering coefficient (μ'_s) for skin [Fig. 3(a)] decreases after 30 min of 50% glycerol exposure and returns to very near its untreated value after rehydration. The absorption coefficient (μ_a) after 30 min of glycerol exposure is nearly the same as in the untreated state [Fig. 3(b)]. The limited thickness of the mouse skin samples ($\sim 220 \mu\text{m}$) causes the inverse-adding doubling (IAD) program to return values that are not meaningful for weakly attenuated wavelengths in the cleared skin samples. Nevertheless, it can still be seen that μ'_s is reduced by approximately one order of magnitude for the wavelengths of interest.

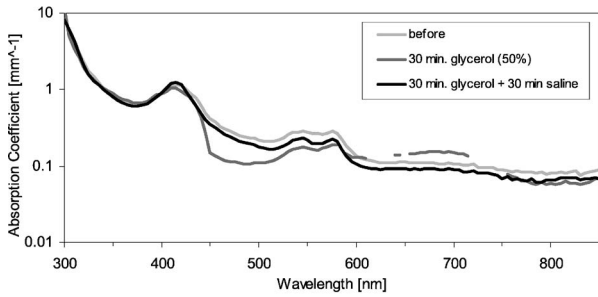
Plots of intensity and spatial resolution for three wavelengths for the simulated bioluminescence experiment are shown in Figs. 4(a) and 4(b). Both values decrease with increasing glycerol (50%) exposure. The maximum intensity decrease after 1800 s was 38.8% for 550-nm light, 48.4% for 600-nm light, and 42.6% for 650-nm light. Spot size decreased by 51.9% for 550-nm light, 60.0% for 600-nm light, and 68.0% for 650-nm light after 1800 s. The measured spot size was smaller for the shorter wavelength light at all time points.

Figure 5 summarizes the spatial resolution data for the simulated bioluminescence study. Two trends are apparent: increasing spot size with decreasing glycerol concentration and increasing spot size with longer wavelength. Notably, 50% and 100% glycerol concentrations result in significantly decreased spot sizes (i.e., better spatial resolution) compared to native tissue ($p < 0.001$) while there is no statistically significant difference between native skin and 25% glycerol-treated skin.

The results of the *in vivo* macroscopic imaging study are shown as Fig. 6. Figure 6(a) shows a section of mouse skin 30 min after injection of 0.2 ml of 100% glycerol. The same



(a)



(b)

Fig. 3 Reduced scattering coefficient (a) and absorption coefficient (b) of *in vitro* normal skin, glycerol treated skin (50%, 30 min), and skin treated with glycerol for 30 min then placed in saline for 30 min. Each line represents the average of three independent measurements ($n=3$). Optical properties were calculated from transmission and reflectance measurements using an IAD program. In the spectral range of interest (550 to 650 nm), the absorption coefficient is unaffected by the glycerol treatment, while the reduced scattering coefficient drops by nearly one order of magnitude.

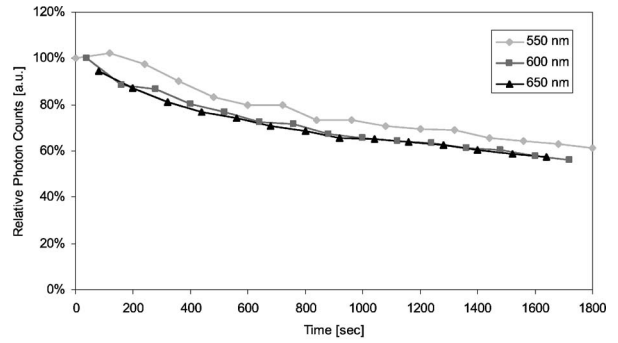
section of skin is shown 24 h later [Fig. 6(b)] when the clearing effects have reversed.

Integrated intensity and spot diameter for the *in vivo* simulated BLI experiment are shown in Figs. 7(a) and 7(b), respectively. Both plots show a decrease of intensity and spot diameter, respectively, as the tissue clears with time.

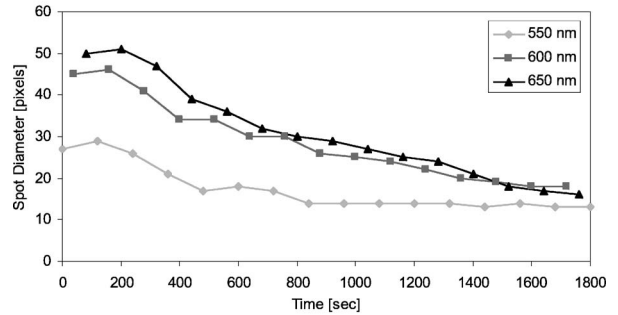
4 Discussion

In this study, we have investigated the use of glycerol as a tissue clearing agent in order to improve the sensitivity and spatial resolution of *in vivo* BLI. To address the feasibility of this approach, we conducted a set of experiments determining the optical properties of skin *in vitro* and designed a set of experiments to study the effects of skin clearing in experiments in which a diffusing fiber tip was used as a simulated and constant (point) source of bioluminescence emission.

The optical properties of mouse skin measured for the skin before treatment, after 30 min of glycerol (50%) exposure, and after rehydration with saline for 30 min (Figs. 2 and 3) were consistent with previous studies on rat skin and hamster skin.²⁶ Tissue optical clearing is believed to be due to a decrease in the reduced scattering coefficient by index matching of extracellular fluid and tissue solid components. Within the spectral range of interest (550 to 650 nm) total (diffuse) transmission increased on average by a factor of 1.70 and diffuse reflectance decreased on average by a factor 3.37. After 30 min of saline rehydration, both transmission and reflectance



(a)



(b)

Fig. 4 Integrated photon intensity (photon counts) (a) and spot diameter (b) measured by the imaging system through skin as a function of time of exposure to glycerol. Both parameters decrease with time (and hence with decreasing the reduced scattering coefficient).

tance values returned to within 10% of their untreated values. This was confirmed by the results of an IAD program, which calculated μ'_s and μ_a from the spectrophotometer data. Over the spectral range of interest, the reduced scattering coefficient (μ'_s) decreased on average by approximately one order of magnitude, while the absorption coefficient (μ_a) was nearly constant (<5% change). The IAD model was unable to compute meaningful results for wavelengths >450 nm in cleared skin due to a combination of low scattering combined with the relatively thin mouse skin thickness. Nevertheless, the reduction in diffuse reflectance, the increase in transmission, and the calculated optical properties in the range where

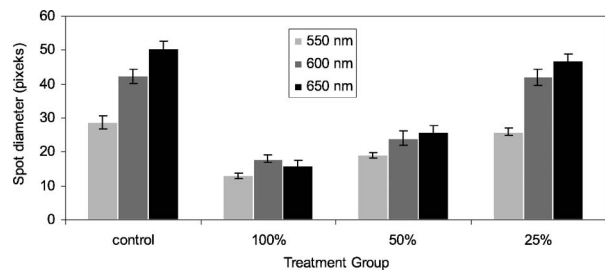
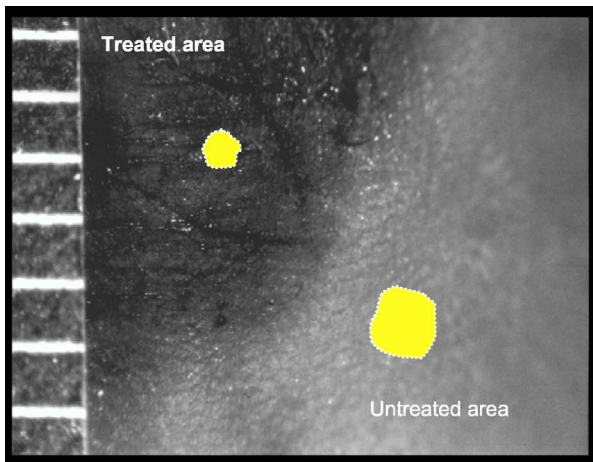
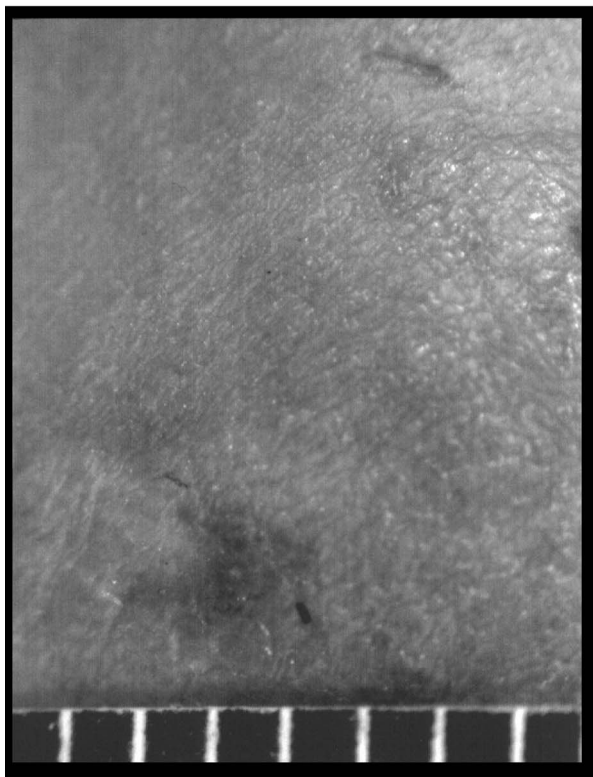


Fig. 5 Effect of glycerol concentration on spot size reduction of skin *in vitro* for different wavelengths. Note that 25% glycerol is ineffective in clearing skin after 30 min and shows values that are not different from native skin. In all cases, the spot size for 650-nm light is larger than that for 550-nm light as expected. However, the change in spot size due to glycerol is most significant at the 650-nm wavelength.



(a)

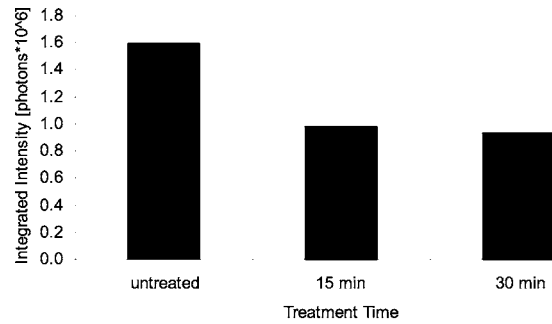


(b)

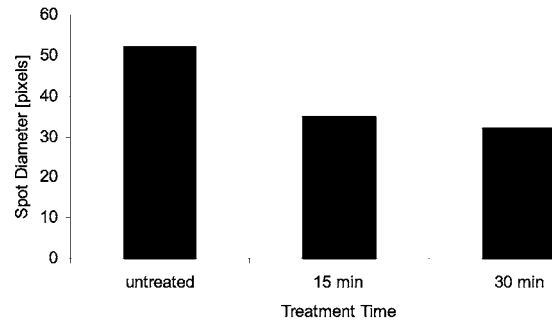
Fig. 6 Image of *in vivo* mouse skin 30 min after injection of 0.2 ml 100% glycerol (a) and 24 h after (b) glycerol application when clearing is reversed. The left top part of the image shows the area where glycerol was applied, the right bottom shows an area of normal skin. The luminescent spot (for 650 nm) thresholded at photon counts >100, generated by the 500- μ m diameter diffusing fiber is shown in (a) in both the cleared and untreated portion of the skin. Note that the spot size reduced by a factor of approximately 2 in cleared skin.

the model did converge are in general agreement with data published on rat and hamster skin.²⁵⁻²⁷

The decrease in light detected by the camera, seen after glycerol application (Fig. 4) in the *in vitro* simulated bioluminescence experiment was unexpected and in apparent conflict with the integrating sphere measurements, which showed a 1.7-fold increase in transmission. However, we speculate that



(a)



(b)

Fig. 7 Effect of glycerol application *in vivo* on integrated photon intensity (a) and spot diameter (b) measured by the imaging system through skin of a live mouse before, at 15 min, and at 30 min of glycerol application. Note that both parameters decrease with time (and hence with decreasing the reduced scattering coefficient) similar to what was seen *in vitro*.

this apparent discrepancy can be explained by the fact that fundamentally the two measurements are different. Traditionally, a double integrating sphere setup is used to measure total transmission and diffuse reflectance. In this setup, all of the light incident on the tissue is accounted for by one sphere or the other. More specifically, with regards to the transmission measurements, all transmitted light (i.e., total transmittance), irrespective of the angle with the tissue normal, is captured in this measurement. Hence, if the reduced scattering coefficient decreases as is the case in skin treated with glycerol, the total attenuation coefficient decreases, and hence, the overall transmission of light through the tissue increases. In contrast, the imaging geometry where the camera is positioned approximately 50 cm above the tissue sample and has an effective aperture of roughly 2.5 cm detects only light that is emitted within the acceptance cone angle of the camera (~ 7 deg). The decrease in light reaching the camera in cleared skin compared to native skin is believed to be due to the reduction of multiple scattering events. In the native skin, light emitted in a direction that would put it outside the camera's acceptance angle can be multiply scattered and redirected to emit from the tissue in a direction within the camera's acceptance angle. The net result of this is a decrease in light detected by the camera (causing a decrease of approximately 40%) when the reduced scattering coefficient of the sample decreases (by a factor of 10), even though the total transmission of light through the sample is increased. We hypothesize that this geometric effect is also responsible for the apparent conflict between our imaging data and data published by Vargas et al.²⁷

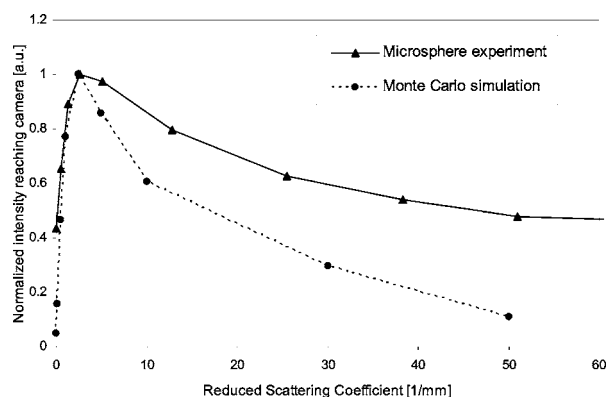


Fig. 8 Photon intensity detected by the imaging system as a function of the reduced scattering coefficient. Experimentally (\blacktriangle), a serial dilution of polystyrene microspheres was made and simulated bioluminescence from the diffusing fiber tip was measured. Simulation results (\bullet) were obtained from Monte Carlo simulations with the appropriate geometry to simulate light collection within the cone angle and aperture of the detector.

who showed increased fluorescence detected when skin was cleared and He et al.,³³ who showed increased signal detection in low light level imaging applications after tissue clearing. In both these studies, different photon collection geometries were used. Vargas et al. used a multifiber probe consisting of 200- μm diameter optical fibers with a NA of 0.2 (acceptance angle ~ 12 deg) in contact with the tissue. In the study by He et al., the imaging geometry was not reported and apparently not considered in their Monte Carlo simulations. In addition, significantly thicker tissue samples were used, making a direct comparison difficult, if not impossible. Nevertheless, both these studies used geometries that are different from the typical BLI setup that employs a 1-in aperture roughly 50 cm away from the tissue surface. We conducted two experiments to verify our multiple scattering hypothesis. First, we imaged the fiber tip under a layer of scattering liquid consisting of polystyrene microspheres (diameter 0.954 μm) in decreasing concentrations (and hence decreasing scattering coefficients). The setup was similar to Fig. 1 but with the tissue layer replaced by scattering liquid. In this experiment (Fig. 8), we found that as μ'_s is increased from 0 to ~ 3 mm^{-1} , light reaching the camera increases. When μ'_s was increased beyond 3 mm^{-1} , light reaching the camera decreases. The net effect of changing the reduced scattering coefficient 10 mm^{-1} (native skin) to < 1 mm^{-1} (cleared skin) is a reduction of light reaching the camera. This is consistent with our observation in native and clear skin. As we continue to increase μ'_s , the slope of the curve changes and light levels reaching the camera start to decrease. The second experiment that was conducted to verify our hypothesis consisted of a Monte Carlo simulation. Using an isotropic light source underneath a slab geometry with the optical properties of normal and cleared skin, we determined the transmitted light as a function of radius and angle. Plots were generated of the light reaching the plane of the camera as function of radius. In this scenario (Fig. 8), we confirmed the data from the microsphere experiments and found that a combination of thin tissue layer, constant μ_a , and a reduction in μ'_s from 10 mm^{-1} to less than 1 mm^{-1} leads to a decrease of light transmission within the

acceptance angle of the camera, despite the fact that the total transmission increases. Although the decrease in intensity was not the desired effect, it may be a tradeoff for the increase in spatial resolution.

Glycerol application caused a decrease in spot size [Fig. 7(a)] ranging from 51.9% for 550 nm light to 68.0% for 650 nm light. The difference in resolution improvement between the wavelengths used is believed to be due to absorption (and hence the shorter mean free path) of shorter wavelength light by hemoglobin. Higher glycerol concentrations were also shown to be more effective at improving spatial resolution at 30 min postinjection (Fig. 5). Notably, 100% and 50% glycerol are effective in reducing the imaged spot size (i.e., increasing spatial resolution), while 25% glycerol was not able to cause changes in spot size that were significantly different from native tissue. This is due to the higher osmotic pressure of the higher concentration of agent.^{26,27}

The *in vivo* macroscopic imaging study (Fig. 6) showed that, in accordance with previous studies, gross subdermal structures normally obscured by turbid tissue can be made visible by treatment with hyperosmotic agent. It was also shown that the clearing effects reversed 12 to 24 h after injection.

Penetration of optical clearing agents through intact skin (*in vivo*) is minimal and extremely slow. This has been attributed to the fact that these agents are hydrophilic and penetrate the lipophilic stratum corneum poorly. In this study, we circumvented this problem by injecting the clearing agent directly in the skin (intradermally). Subdermal injections had no noticeable clearing effects. Given the relatively small thickness of the tissue (≈ 220 μm), it is difficult to inject the necessary amount (0.2 ml) of glycerol. It was found that relatively high glycerol concentrations (50 to 100%) were necessary to achieve clearing within the desired time frame (15 to 30 min). At this concentration, the solution has a high viscosity, further increasing the difficulty of injection.

Promising recent work by Khan et al., who have explored a number of different skin clearing agents, has shown that a combination of Food and Drug Administration–approved lipophilic PPG based polymers and hydrophilic PEG is an effective, topically applied skin clearing agent. Although we have not tried this agent in mice, *in vitro* and *in vivo* results in humans suggest that it does not have the problems associated with glycerol.²⁸

The results of the *in vivo* simulated bioluminescence experiment [Figs. 7(a) and 7(b)] were consistent with the trends seen in the *in vitro* experiments (Figs. 4 and 5). A 41.8% decrease in integrated intensity and a 38.5% decrease in spot size were seen 30 min postinjection. Although we limited our tissue clearing to the clearing of skin for practical reasons (it is difficult to obtain adequate diffusion of the agent in thicker layers, especially *in vivo*), BLI is particularly useful for the imaging of processes that occur several millimeters or even centimeters below the tissue surface. For those cases, clearing only the skin (200 to 300 μm in thickness in a typical mouse) will have a significantly reduced effect. Nevertheless, it is conceivable to extend this approach to clearing deeper tissues layers, in which case, spatial resolution is significantly improved and evidence suggests that the photon flux may in fact be improved,³³ depending on the imaging geometry.

5 Conclusions

In summary, we have shown that applying a hyperosmotic clearing agent to skin of small rodents has the potential to improve spatial resolution of BLI owing to a reduction in the reduced scattering coefficient in skin by one order of magnitude. In contrast, reducing the scattering coefficient reduces the amount of light reaching the camera due to a reduction in the amount of multiple scattered light that reaches the camera aperture and thus reducing sensitivity of the method. Tissue thickness and imaging geometry appear to be the critical factors that determine the effect of tissue clearing on spatial resolution and sensitivity.

Acknowledgments

The authors want to thank Dr. Rudolph Verdaasdonk (Utrecht University, The Netherlands) for providing the diffusing fiber tip used in these experiments. Funding for this research was provided by grants from the Vanderbilt In Vivo Imaging Center (VIVID) (No. NIH P20 CA86283), the Diabetes Center Pilot and Feasibility Project (No. NIH-NIDDK P60 DK20593), and the NSF Research Experience for Undergraduates (REU) (No. EEC-9820566).

References

1. D. A. Benaron, P. R. Contag, and C. H. Contag, "Imaging brain structure and function, infection and gene expression in the body using light," *Philos. Trans. R. Soc. London, Ser. B* **352**(1354), 755–61 (1997).
2. R. T. Sadikot, E. D. Jansen, T. R. Blackwell, O. Zoia, F. Yull J. W. Christman, and T. S. Blackwell, "High-dose dexamethasone accentuates nuclear factor-kappa b activation in endotoxin-treated mice," *Am. J. Respir. Crit. Care Med.* **164**(5), 873–78 (2001).
3. C. H. Contag, S. D. Spilman, P. R. Contag, M. Oshiro, B. Eames, P. Denery, D. K. Stevenson, and D. A. Benaron, "Visualizing gene expression in living mammals using a bioluminescent reporter," *Photochem. Photobiol.* **66**(4), 523–31 (1997).
4. C. H. Contag, D. Jenkins, P. R. Contag, and R. S. Negrin, "Use of reporter genes for optical measurements of neoplastic disease in vivo," *Neoplasia* **2**(1–2), 41–52 (2000).
5. R. T. Sadikot, L. J. Wudel, D. E. Jansen, J. P. Debelak, F. E. Yull, J. W. Christman, T. S. Blackwell, and W. C. Chapman, "Hepatic cryoablation-induced multisystem injury: bioluminescent detection of NF-kappaB activation in a transgenic mouse model," *J. Gastrointest Surg.*, **6**(2), 264–70 (2000).
6. N. Wu, S. Opalenik, J. Liu, E. D. Jansen, M. G. Giro, and J. M. Davidson, "Real-time visualization of MMP-13 promoter activity in transgenic mice," *Matrix Biol.* **21**(2), 149–61 (2002).
7. N. J. Wu, E. D. Jansen, and J. M. Davidson, "Comparison of MMP-13 Expression In Free-Electron Laser and Scalpel Incisions During Wound Healing," *J. Invest. Dermatol.* **21**(4), 926–32 (2003).
8. C. H. Contag, P. R. Contag, J. I. Mullins, S. D. Spilman, D. K. Stevenson, and D. A. Benaron, "Photonic detection of bacterial pathogens in living hosts," *Mol. Microbiol.* **18**(4), 593–603 (1995).
9. G. R. Siragusa, K. Nawotka, S. D. Spilman, P. R. Contag, and C. H. Contag, "Real-time monitoring of Escherichia coli O157:H7 adherence to beef carcass surface tissues with a bioluminescent reporter," *Appl. Environ. Microbiol.* **65**(4), 1738–45 (1999).
10. H. L. Rocchetta et al., "Validation of a noninvasive, real-time imaging technology using bioluminescent Escherichia coli in the neutropenic mouse thigh model of infection," *Antimicrob. Agents Chemother.* **45**(1), 129–37 (2001).
11. K. P. Francis, D. Joh, C. Bellinger-Kawahara, M. J. Hawkinson, T. F. Purchio, and P. R. Contag, "Monitoring bioluminescent Staphylococcus aureus infections in living mice using a novel luxABCDE construct," *Infect. Immun.* **68**(6), 3594–600 (2000).
12. K. P. Francis et al., "Visualizing pneumococcal infections in the lungs of live mice using bioluminescent Streptococcus pneumoniae transformed with a novel gram-positive lux transposon," *Infect. Immun.* **69**(5), 3350–58 (2001).
13. G. D. Luker and D. A. Leib, "Luciferase real-time bioluminescence imaging for the study of viral pathogenesis," *Methods Mol. Biol.* **292**, 285–96 (2005).
14. P. R. Contag, I. N. Olomu, D. K. Stevenson, and C. H. Contag, "Bioluminescent indicators in living mammals," *Nat. Med.* **4**(2), 245–47 (1998).
15. A. Rehemtulla, L. D. Stegman, S. J. Cardozo, S. Gupta, D. E. Hall, C. H. Contag, and B. D. Ross, "Rapid and quantitative assessment of cancer treatment response using *in vivo* bioluminescence imaging," *Neoplasia* **2**(6), 491–95 (2000).
16. M. Edinger, T. J. Sweeney, A. A. Tucker, A. B. Olomu, R. S. Negrin, and C. H. Contag, "Noninvasive assessment of tumor cell proliferation in animal models," *Neoplasia* **1**(4), 303–10 (1999).
17. T. J. Sweeney, V. Mailander, A. A. Tucker, A. B. Olomu, W. Zhang, Y. Cao, R. S. Negrin, and C. H. Contag, "Visualizing the kinetics of tumor-cell clearance in living animals," *Proc. Natl. Acad. Sci. U.S.A.* **96**(21), 12044–49 (1999).
18. M. Vooijs, J. Jonkers, S. Lyons, and A. Berns, "Noninvasive imaging of spontaneous retinoblastoma pathway-dependent tumors in mice," *Cancer Res.* **62**(6), 1862–67 (2002).
19. A. Wetterwald et al., "Optical imaging of cancer metastasis to bone marrow: a mouse model of minimal residual disease," *Am. J. Pathol.* **160**(3), 1143–53 (2002).
20. M. L. Koransky, T. K. Ip, S. Wu, Y. Cao, G. Berry, C. Contag, H. Blau, and R. Robbins, "In vivo monitoring of myoblast transplantation into rat myocardium," *J. Heart Lung Transplant* **20**(2), 188–189 (2001).
21. M. Fowler et al., "Assessment of pancreatic islet mass after islet transplantation using *in vivo* bioluminescence imaging," *Transplantation* **79**(7), 768–76 (2005).
22. T. Wilson and J. W. Hastings, "Bioluminescence," *Annu. Rev. Cell Dev. Biol.* **14**, 197–230 (1998).
23. B. W. Rice, M. D. Cable, and M. B. Nelson, "In vivo imaging of light-emitting probes," *J. Biomed. Opt.* **6**(4), 432–40 (2001).
24. H. Zhao, T. C. Doyle, O. Coquoz, B. W. Rice, and C. H. Contag, "Emission spectra of bioluminescent reporters and interaction with mammalian tissue determine the sensitivity of detection *in vivo*," *J. Biomed. Opt.* **10**(4), 41210 (2005).
25. V. V. Tuchin, I. L. Maksimova, D. A. Zimnyakov, I. L. Kon, A. H. Mavlyutov, and A. A. Mishin, "Light propagation in tissues with controlled optical properties," *J. Biomed. Opt.* **2**(4), 401–17 (1997).
26. G. Vargas, E. K. Chan, J. K. Barton, H. G. Rylander, III, and A. J. Welch, "Use of an agent to reduce scattering in skin," *Lasers Surg. Med.* **24**(2), 133–41 (1999).
27. G. Vargas, K. F. Chan, S. L. Thomsen, and A. J. Welch, "Use of osmotically active agents to alter optical properties of tissue: effects on the detected fluorescence signal measured through skin," *Lasers Surg. Med.* **29**(3), 213–20 (2001).
28. M. H. Khan, B. Choi, S. Chess, M. K. K. J. McCullough, and J. S. Nelson, "Optical clearing of *in vivo* human skin: implications for light-based diagnostic imaging and therapeutics," *Lasers Surg. Med.* **34**(2), 83–85 (2004).
29. M. H. Khan, S. Chess, B. Choi, K. M. Kelly, and J. S. Nelson, "Can topically applied optical clearing agents increase the epidermal damage threshold and enhance therapeutic efficacy?" *Lasers Surg. Med.* **35**(2), 93–95 (2004).
30. B. Choi, L. Tsu, E. Chen, T. S. Ishak, S. M. Iskandar, S. Chess, and J. S. Nelson, "Determination of chemical agent optical clearing potential using *in vitro* human skin," *Lasers Surg. Med.* **36**(2), 72–75 (2005).
31. V. V. Tuchin, X. Xu, and R. K. Wang, "Dynamic optical coherence tomography in studies of optical clearing, sedimentation, and aggregation of immersed blood," *Appl. Opt.* **41**(1), 258–71 (2002).
32. S. A. Prahl, "The adding-doubling method," in *Optical-Thermal Response of Laser-Irradiated Tissue*, A. J. Welch and M. J. C. van Gemert, Eds., pp. 101–25, Plenum Press, New York (1995).
33. Y. He and R. K. Wang, "Improvement of low-level light imaging performance using optical clearing method," *Biosens. Bioelectron.* **20**(3), 460–67 (2004).